Excerpt from the Proceedings of the 2011 COMSOL Conference in Stuttgart

The Effect of the Disintegration of Chemical Stratification on the Time-dependent Behavior of the Earth’s Mantle

Attila Galsa[*,1] and Mátyás Herein[1]
[1]Department of Geophysics and Space Science, Eötvös University
*Pázmány Péter str. 1/C., Budapest, Hungary, H-1117, gali@pangea.elte.hu

Abstract: Numerical calculations have been carried out in order to investigate the effect of the chemically dense D’’ layer on the time-dependent behavior of the Earth’s mantle. The D’’ layer around the Earth’s core intensively influences the heat flow, velocity, temperature and concentration of dense material, larger density contrast has stronger and/or longer effect on the parameters. The evolution of the D’’ layer can be well correlated with the time series of the parameters monitored during the simulation. The disintegration and mixing of the dense layer can be predicted by the reinterpreted buoyancy ratio. The time-dependent behavior of the buoyancy ratio can be deduced from three main reasons: (1) the heat coming from the core warms up the dense layer reducing its density by thermal expansion, (2) the thermal convection evolving in the upper layer erodes the surface of the dense layer and (3) the thermal convection forming in the D" layer intermixes the light material from the overlaying zone.

Keywords: geodynamics, mantle convection, thermo-chemical plumes, D’’ layer.

1. Introduction

The existence of D’’ layer above the Earth’s core-mantle boundary (CMB) with a thickness of about 200–300 km has been widely known for the last decades. Already in the first part of the 20th century it has been identified as a low/negative seismic gradient of P and S wave velocities in the early radial Earth’s models compiled by Gutenberg [1], Jeffreys and Bullen [2]. Since that time numerous physical manifestations of the D’’ layer have been hypothesized, revealed or verified such as the temperature drop in the lower thermal boundary layer [3], the chemical density increase [4], the exotherm phase transition from perovskite to post-perovskite [5], ultra low velocity zone [6], anisotropy [7], topography [8, 9] etc.

Beyond the complexity of the D’’ layer, it is not questionable, that this zone is one the most exciting part of the Earth in terms of geodynamics. According to different conceptions the D’’ layer is both the birth-place of mantle upwellings/plumes and the graveyard of subducting plates, at least partly. The chemically distinct property has an additional role on the flow system evolving from/within the layer. The thermal plumes forming in chemically homogeneous mantle are fed by heat coming from the Earth’s core across the bottom thermal boundary layer (TBL). However, if the lowest part of the mantle has larger density, it is able to reduce the heat flux from the core, to cool the mantle, to slow down and stabilize the flow that is to vary the flow regime of the whole mantle.

The single parameter varied during the simulation is the relative density difference between the D’’ layer and the overlaying mantle. A number of parameters characterizing the mantle convection were monitored such as heat flux on the surface, at the CMB and the top of D’’ layer; root-mean-square velocities, temperatures and the concentration in different zones of the mantle, as well as concentration flux and the heterogeneity of the dense material.

2. Numerical model

2.1 Mathematical background

The Boussinesq approximation of the equation system governing the thermo-chemical convection was applied. The equations expressing the conservation of the mass, the momentum as well as the heat and the mass transport are

$$\frac{\partial u_i}{\partial x_i} = 0, \tag{1}$$

$$\frac{du_i}{dt} = ge_i - \frac{\partial p}{\partial x_i} + \frac{\partial \;_{ij}}{\partial x_j}, \tag{2}$$

$$\frac{\partial T}{\partial t} = \frac{\partial^2 T}{\partial x_i^2} - u_i \frac{\partial T}{\partial x_i}, \tag{3}$$

$$\frac{\partial c}{\partial t} = D\frac{\partial^2 c}{\partial x_i^2} - u_i \frac{\partial c}{\partial x_i}, \tag{4}$$

where the unknown variables are the density, the pressure, the flow velocity, the temperature of the fluid and the concentration of the dense material, , p, u_i, T and c, respectively. In two-dimensional model domain there are five equations to determine six variables. Therefore a simple linear relation is given among density, the temperature and the concentration by the equation of state,

$$= {}_{\boldsymbol{S}}\left[1- \ \left(\boldsymbol{T}-\boldsymbol{T_S}\right)+ \ \boldsymbol{c}\right], \qquad (5)$$

where $_{\boldsymbol{S}}$ and $\boldsymbol{T_S}$ denotes surface density and temperature, is the initial relative density difference between the D’’ layer and the overlaying mantle. Newtonian, viscous rheology was applied for the mantle, thus the stress tensor in case of incompressible fluid is

$$_{ij} = \left[\frac{\partial \boldsymbol{u_i}}{\partial \boldsymbol{x_j}} + \frac{\partial \boldsymbol{u_j}}{\partial \boldsymbol{x_i}}\right]. \qquad (6)$$

According to the Boussinesq approximation other parameters in the (1)–(6) equation system are supposed to be constant (***Table 1***). Analogously, the density of the fluid is constant in each term, apart from the buoyancy force (1st term in the right side of (2)) in order to ensure the influence of the temperature and the concentration on the flow system via the Navier-Stokes equation. The space coordinates and the time are denoted by $\boldsymbol{x_i}$ and $\boldsymbol{t}$, respectively; $\boldsymbol{e_i}$ shows the direction of the gravitational acceleration, downwards.

Table 1: Mantle parameters in model

gravitational acceleration	g	9.92 m/s^2
dynamic viscosity	η	2·10^{21} Pas
heat diffusivity	κ	10^{-6} m^2/s
diffusion coefficient	$\boldsymbol{D}$	10^{-11} m^2/s
coefficient of thermal expansion	α	2·10^{-5} 1/K
surface density	$_{\boldsymbol{s}}$	4500 kg/m^3

The exact values of the physical parameters in Table 1 are rather poorly known for the Earth’s mantle. In order to reduce the inaccuracy, conventionally, non-dimensional equations are introduced. In Boussinesq-approximation there are only one non-dimensional number governing the thermal convection, the Rayleigh number. The Rayleigh number is

$$\boldsymbol{Ra} = \frac{'\boldsymbol{buoyancy\ force}'}{'\boldsymbol{viscous\ force}'} = \frac{{}_{\boldsymbol{s}} \ \boldsymbol{g}\Delta \boldsymbol{T}\boldsymbol{d}^3}{}, \qquad (7)$$

where the viscous force is the last term of (2); $\Delta\boldsymbol{T}=\boldsymbol{T_{CMB}}-\boldsymbol{T_S}$ is the temperature difference between the core-mantle boundary (CMB) and the surface, and $\boldsymbol{d}$=2900 km means the thickness of the mantle. It is presumed that the value of the Rayleigh number for the Earth’s mantle is in the order of magnitude of 10^7. In order to calibrate our calculations to $\boldsymbol{Ra}=10^7$, $\Delta\boldsymbol{T} \cong 918.5\ \boldsymbol{K}$ was applied during the simulation which is probably less than the real temperature drop.

2.1 Model description

Two-dimensional cylindrical shell geometry was used to imitate the shape of the Earth’s mantle with an outer and inner radius of 6370 km and 3470 km, respectively. The initial thickness of the D’’ layer was 300 km around the core. The outer boundaries were isothermal as well as symmetrical and impermeable in point of the velocity and the concentration. Interior boundary (top of D’’) was continuous.

Simulation was started from a quasi-stationary state of the temperature field obtained from a chemically homogeneous, purely thermal convection model. Concentration of dense material was set to 1 in D’’ and 0 above, the transition was adjusted using smoothed Heaviside function with continuous first derivative (flc1hs) and interval thickness of 50 km.

Triangle (advancing front) finite element was applied to mesh the domain with a maximum size of 75 km in the subdomains, 50 km along the surface and 25 km along the CMB and the top of D’’, which resulted in 73772 elements. In the interior of elements Lagrange P_2-P_1, Lagrange quadratic and Lagrange cubic shape functions were used to approximate the solution of the velocity, the temperature and the concentration, respectively.

In order to minimize the number and size of over/undershots in the concentration field ($\boldsymbol{c}>1$ or $\boldsymbol{c}<0$) artificial diffusion was utilized. All the streamline (Petrov-Galerkin/ Compensated), crosswind (Shock Capturing) and isotropic diffusion were put on, latter only in over/undershots (($\boldsymbol{c}>1.04$)+($\boldsymbol{c}<-0.04$)) to reduce the artificial intervention. The influences of the artificial diffusion on the model were extensively tested to avoid the distortion of the result.

The single parameter modified during the simulation was the relative density difference, between the dense D’’ layer and the lighter overlaying mantle, it ranged between 0.1–3%. In the following section the effect of on the variations in the time-series of monitored parameters and the evolution of the D’’ layer will be analyzed.

3. Results

A dense layer at the bottom of the mantle is expected to hinder the convection by reducing the vertical heat advection from the Earth’s core. Therefore the chemically dense D’’ layer has a stabilizing role. On the other hand, the heat coming from the core is trapped that leads to a hot that is unstable bottom thermal boundary layer (TBL). The winner from the two contrary effects can be predicted defining the buoyancy ratio,

$$\boldsymbol{B} = \frac{\quad}{\Delta \boldsymbol{T}}, \tag{8}$$

which is the ratio of the stabilizing chemical density difference and the destabilizing thermal density difference. When ***B*** is larger than one, the dense layer is thought to be stable, but in case of ***B***<1, the density decrease by thermal expansion seems to be strong enough to ‘dissolve’ the D’’. In this meaning of the buoyancy ratio it is not difficult to anticipate that larger relative chemical density contrast, requires more stable D’’ layer. ***Figure 1*** illustrates the effect of or ***B***.

It is obvious that 600 Myr is long enough to break up the D’’ layer when <1%, although this time period seems too short to homogenize it perfectly. In case of =1% the disintegration has occurred, domes or piles are developed from the layer which feed the overlaying mantle with hot, chemically dense

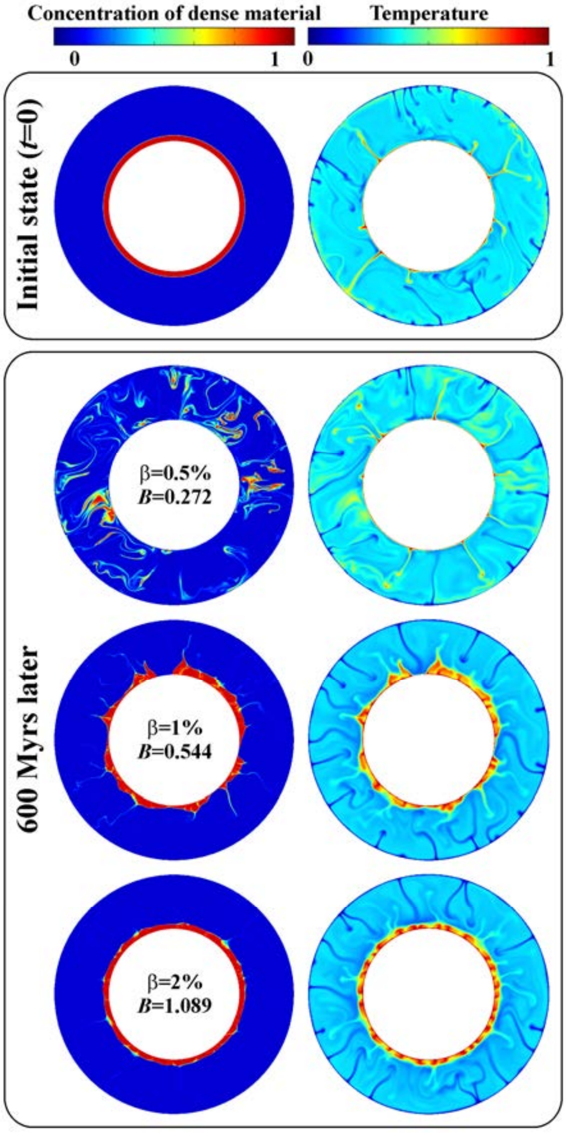

Figure 1. The concentration of the dense material and the temperature at the initial state (***t***=0) and ***t***=600 Myrs later at different density contrast ( ) between the D" zone and the overlaying mantle.

material. 600 Myr is too short to develop considerable thermo-chemical plume activity at =2%, merely the topography of D’’ is deformed slightly.

Different heat flux, velocity, temperature and concentration time series (***Table 2***) were monitored during the simulation to analyze the relation between characteristic variations in the

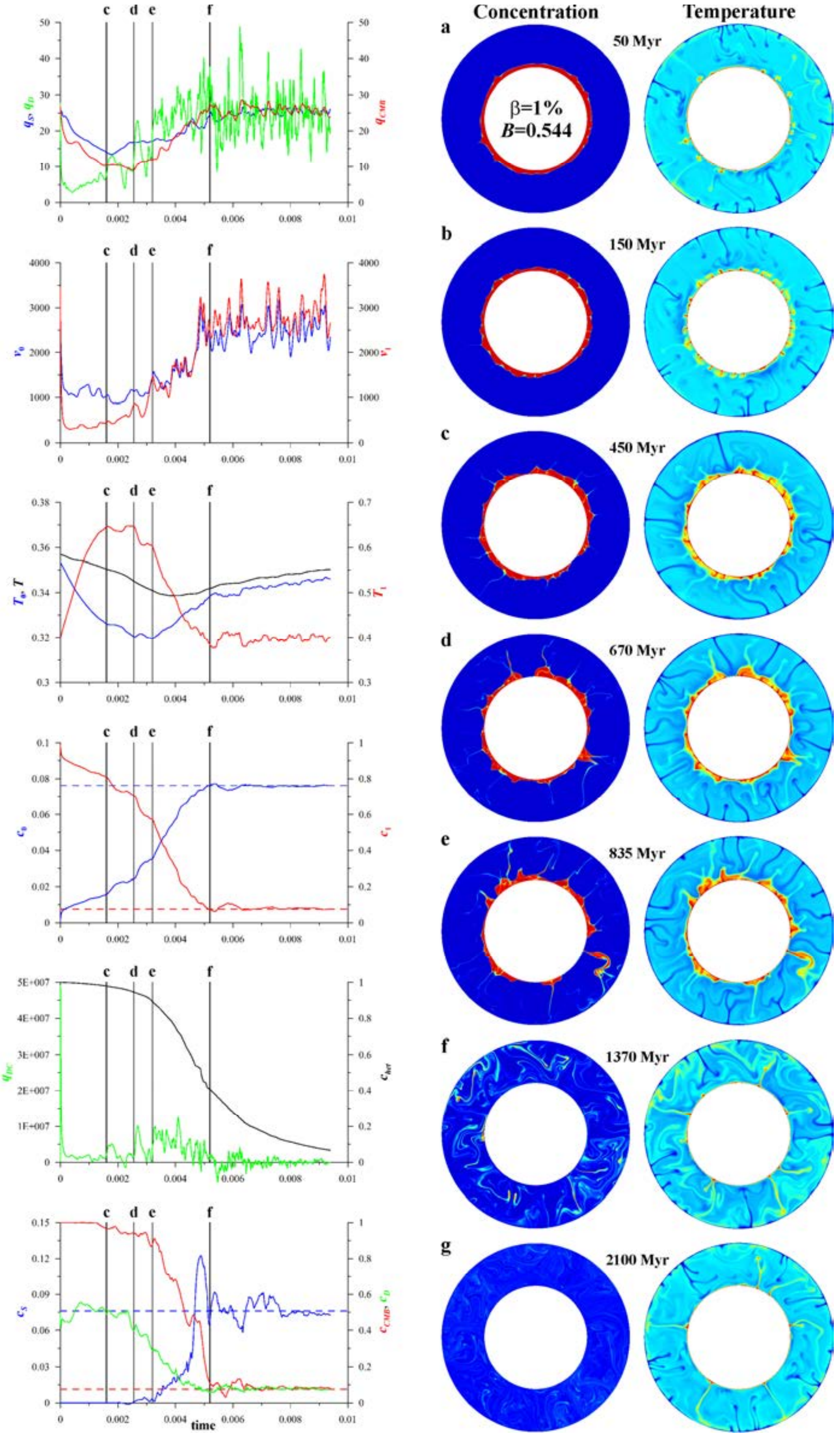

Figure 2. Seven stages of the thermo-chemical evolution of the D’’ layer at =1%. Left: Time series of monitored parameters (see Table 2); right: snapshots of the concentration and the temperature field.

physical parameters and the evolution of D'' layer. Time series were calculated in different subdomains (D'', overlaying mantle) or at boundaries (surface, top of D'', CMB) and were non-dimensionalized in conventional way. D'' layer is defined geometrically as the bottom 300 km of the mantle.

The heterogeneity function of the dense material was computed as

$$\boldsymbol{c_{het}} = \sqrt{\frac{1}{\boldsymbol{V}}\int_{V}\left(\boldsymbol{c}-\bar{\boldsymbol{c}}\right)^{2}\boldsymbol{dV}}\,, \tag{9}$$

where $\boldsymbol{V}$ is the volume of the mantle and the mean concentration of the dense material is

$$\bar{\boldsymbol{c}} = \frac{1}{\boldsymbol{V}}\int_{V}\boldsymbol{c}\,\boldsymbol{dV} = 0.07612\,\cdot \tag{10}$$

It means that $\boldsymbol{c_{het}}$ function has a maximum (1 after normalization) in the initial state and decreases with time by homogenization processes.

In ***Figure 2*** the seven stages of the mixing are shown which could be separated visually:

a deformation of D" layer;
b developed two-layer thermal convection;
c disintegration of D";
d onset of one-layer thermo-chemical convection;
e first dome ceased;
f last dome ceased / mixed mantle;
g homogeneous mantle.

Four stages from the seven are denoted by vertical black line in the graphs of Figure 2 to emphasize the correlation between the computed time series (left) and the evolution of D'' layer (right). (c) At the beginning of disintegration: the temperature increase in D'' stops ($\boldsymbol{T}_1$), the concentration of dense material within D'' decreases more rapidly ($\boldsymbol{c}_1$), the vertical heat and concentration transport at the top of D'' jumps up ($\boldsymbol{q_D}$, $\boldsymbol{q_{DC}}$). (d) At the onset of effective one-layer thermo-chemical convection: the temperature of D'' decreases ($\boldsymbol{T}_1$); the heat flow at CMB increases ($\boldsymbol{q_{CMB}}$); the vertical heat and concentration transport jumps up again ($\boldsymbol{q_D}$, $\boldsymbol{q_{DC}}$). (e) While the first dome is ceasing: D'' cools ($\boldsymbol{T}_1$); the overlaying mantle heats up ($\boldsymbol{T}_0$); the concentration in D'', at CMB and the heterogeneity of the mantle decreases rapidly ($\boldsymbol{c}_1$, $\boldsymbol{c_{CMB}}$, $\boldsymbol{c_{het}}$); the velocities, the heat and concentration flux rise ($\boldsymbol{v}_0$, $\boldsymbol{v}_1$, $\boldsymbol{q_D}$, $\boldsymbol{q_{DC}}$). (f) After the last pile ceased: most of parameters reaches quasi-stationary state (e.g. $\boldsymbol{q_S}$, $\boldsymbol{q_{CMB}}$, $\boldsymbol{v}_0$, $\boldsymbol{v}_1$); the concentration time series achieve the average value, 0.07612 (see (10)); the slope of heterogeneity reduces ($\boldsymbol{c_{het}}$). (g) In the nearly homogeneous mantle the fluctuation of concentration time series decays ($\boldsymbol{c}_0$, $\boldsymbol{c_D}$, $\boldsymbol{c}_1$); the heterogeneity decreases below 10% ($\boldsymbol{c_{het}}$).

Time series of observed and calculated parameters characterizing the nature of the convection reveal unambiguously that the D'' layer around the Earth's core considerably influences the flow system (***Figure 3***). Depending on the relative density contrast, the dense layer stabilizes the flow system and reduces the velocity within D'' ($\boldsymbol{v}_1$), thus the bottom heat warms up the layer ($\boldsymbol{T}_1$) which leads to the reduction of the heat flux from the core ($\boldsymbol{q_{CMB}}$). Less inlet heat results in less outlet heat on the surface ($\boldsymbol{q_S}$) and cooler mantle ($\boldsymbol{T}_0$). Larger density contrast has stronger and/or longer effect on the parameters.

If the density of D'' is small enough, for example due to its high temperature, the layer becomes instable, one-layer thermo-chemical convection starts. By the mixing of the dense material (enhanced concentration flux – $\boldsymbol{q_{DC}}$) the concentration in D'' and at CMB decreases rapidly ($\boldsymbol{c}_1$, $\boldsymbol{c_{CMB}}$), while the concentration increases in the upper zone ($\boldsymbol{c}_0$, $\boldsymbol{c}_{\mathrm{S}}$). Finally, the heat flux, temperature, velocity time-series converge to their original state which is typified by purely thermal convection (black line). On the other hand, the concentration of the dense material tends toward the mean value in each zone of the mantle, the heterogeneity (not shown) decreases toward zero as a perfectly homogeneous final state.

The observation of the time-dependent behavior of the chemically dense D'' layer

Table 2: Observed and calculated non-dimensional parameters

$\boldsymbol{q_S}$	surface heat flow	$\boldsymbol{q_{CMB}}$	heat flow at CMB	$\boldsymbol{q_D}$	heat flow at the top of D''
$\boldsymbol{v}_0$	rms velocity in the upper layer	$\boldsymbol{v}_1$	rms velocity in D''	$\boldsymbol{v}$	rms velocity of the mantle
$\boldsymbol{T}_0$	temperature in the upper layer	$\boldsymbol{T}_1$	temperature in D''	$\boldsymbol{T}$	temperature of the mantle
$\boldsymbol{c}_0$	concentration in the upper layer	$\boldsymbol{c}_1$	concentration in D''	$\boldsymbol{c_{het}}$	heterogeneity of the concentration
$\boldsymbol{c_S}$	concentration at the surface	$\boldsymbol{c_D}$	concentration at the top of D''	$\boldsymbol{q_{DC}}$	concentration flux at the top of D''
$\Delta\boldsymbol{c}$	concentration difference between the upper layer and D''	$\Delta\boldsymbol{T}$	temperature difference between the upper layer and D''	$\boldsymbol{B}$	buoyancy ratio

provides an opportunity to reinterpret the definition of the buoyancy ratio (8). $\boldsymbol{B}$ – in its new meaning – changes in time as the concentration difference ($\Delta \boldsymbol{c}$) and the temperature difference ($\Delta \boldsymbol{T}$) varies between D'' and the overlaying mantle,

$$\boldsymbol{B}(\boldsymbol{t}) = \frac{\Delta \boldsymbol{c}(\boldsymbol{t})}{\Delta \boldsymbol{T}(\boldsymbol{t})}. \tag{11}$$

In this more general interpretation of the buoyancy ratio the effective mixing (in the form of one-layer thermo-chemical plume activity) starts at the value of $\boldsymbol{B} \cong 1$. From this stage it decreases rapidly toward zero, to the death of the D'' layer. Temporarily negative values of $\boldsymbol{B}$ can appear, when the concentration of the dense material is larger in the upper part of the mantle. In the future, applying a more exact analysis the overturn time periods of the thermo-chemical convection can be determined from the concentration time-series (eg. $\Delta \boldsymbol{c}$, $\boldsymbol{c}_1$).

4. Summary and conclusions

Thermo-chemical convection occurring in the Earth's mantle has been modeled numerically in two-dimensional cylindrical shell geometry using the software Comsol Multiphysics. It was established that

1. the existence of the dense D'' layer around the core influences considerably the time-dependent parameters (heat flux, velocity, temperature, concentration) characterizing the flow regime. Larger density contrast has stronger and/or longer effect on the parameters.
2. A good correlation was found between the evolution of D'' layer and the time-series of the parameters monitored during the simulation.
3. A new interpretation of the buoyancy parameter was offered to help the understanding of the thermo-chemical process in the mantle.

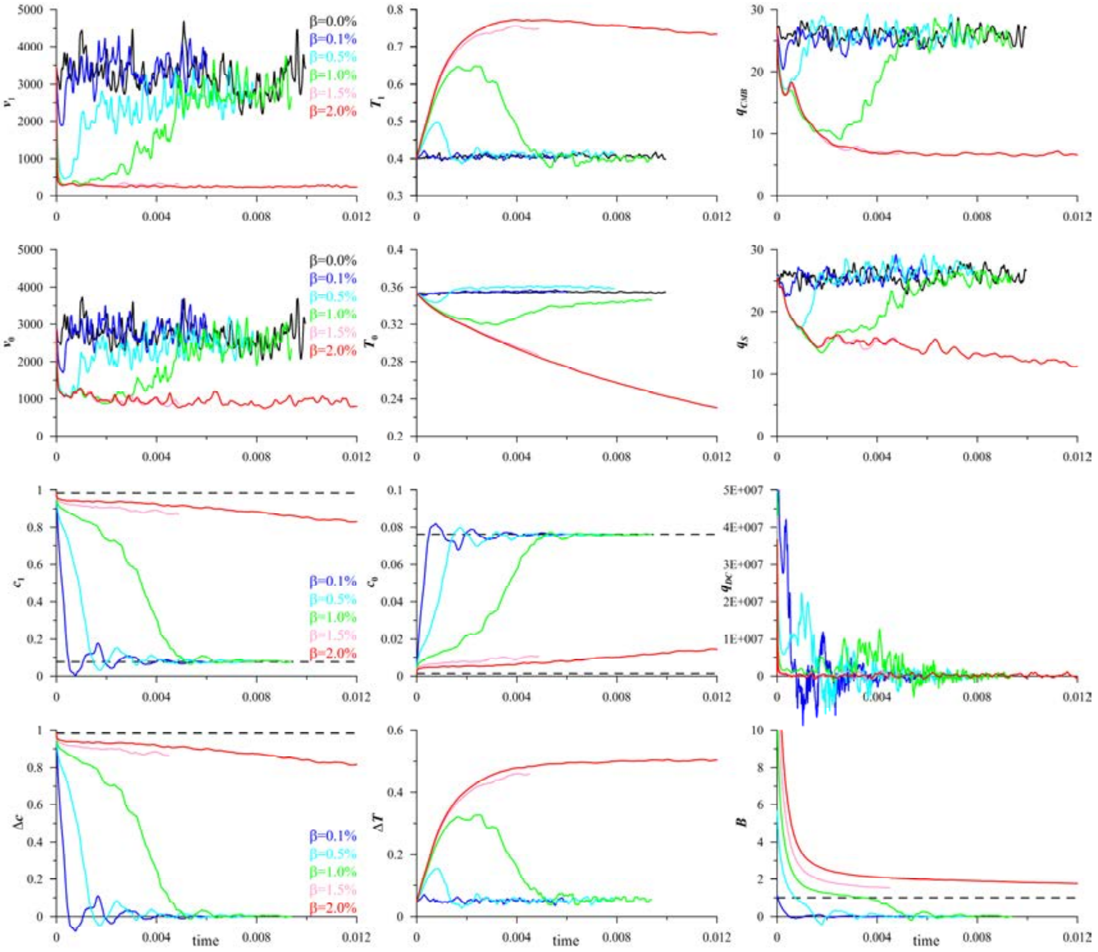

Figure 3. Time series of monitored parameters at different relative density contrasts between the D'' and the overlaying mantle.

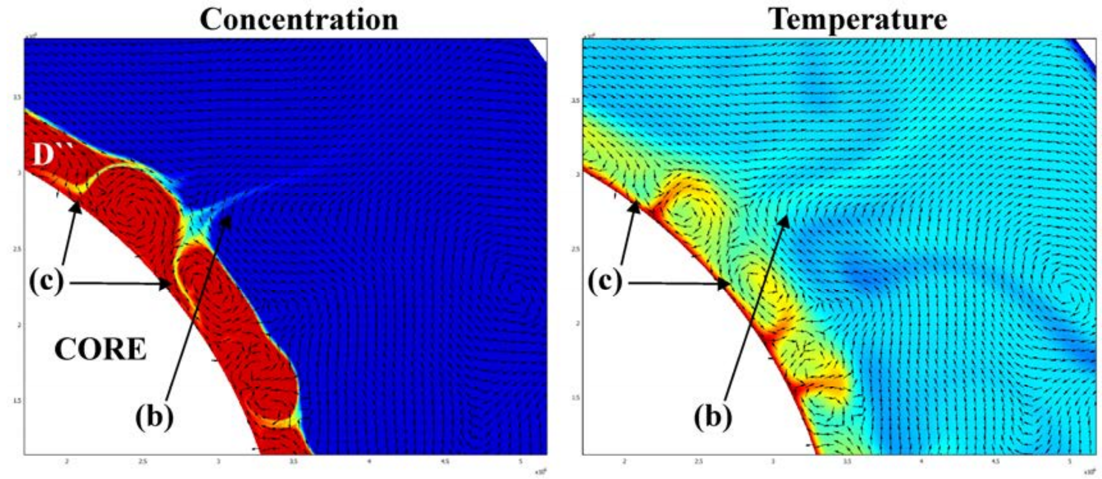

Figure 4. Two processes decreasing the chemical density difference between D’’ and the overlaying mantle. Velocity is indicated by black arrows. (b) Convective pollution of the upper zone with dense material by erosion and (c) dilution of D’’ with light material intermixed from the overlaying zone.

In the latter case the reduction in ***B*** can be deduced from three main reasons based on our quantitative observations:

a the heat coming from the core warms up the dense layer reducing its density by thermal expansion,

b the thermal convection evolving in the upper layer erodes the surface of the dense layer,

c the thermal convection forming in the D" layer intermixes the light material from the overlaying zone.

The first phenomenon increases the thermal buoyancy force (denominator of ***B***), the latter two phenomena (***Figure 4***) decrease the chemical density contrast between the two zones of the mantle (numerator of ***B***). While the process (a) is restricted by the total temperature drop through the mantle, the latter two are not. Thus the pollution of the overlaying zone by dense material as well as the dilution of the D" layer will induce a one-layer thermo-chemical convection that is the ceasing of the dense layer around the Earth's core. Nevertheless, in the cases of ***B***>1 (>2%) the time needed for the disintegration might exceed the age of the Earth.

5. References

1. Gutenberg, B., Über Erdbebenwellen VIIA, ***Kgl. Ges. D. Wiss. Nachr. Heft***, **2**, 125–177 (1914).

2. Bullen, K. E., Compressibility–pressure hypothesis and the Earth’s interior, ***Mon. Not. R. Astron. Soc., Geophys. Suppl.***, **5**, 355–368 (1949).

3. Schubert, G., D. L. Turcotte, P. Olson, ***Mantle Convection in the Earth and Planets***, pp. 940, Cambridge Univ. Press, Cambridge (2001).

4. Manga, M., R. Jeanloz, Implications of a metal-bearing chemical boundary layer in D’’ for mantle dynamics, ***Geophys. Res. Lett.***, **23/22**, 3091–3094 (1996).

5. Hirose, K., Perovskite phase transition and its geophysical implications, ***Rev. Geophys.***, **44**, 2005RG000186 (2005).

6. Jellinek, A. M., M. Manga, Links between long-lived hot spots, mantle plumes, D’’, and plate tectonics, ***Rev Geophys.***, **42**, 2003RG000144 (2004).

7. Thomas, C., J. Wookey, J. Brodholt, T. Fieseler, Anisotropy as cause for polarity reversals of D’’ reflections, ***Earth Planet. Sci. Lett.***, **307**, 369–376 (2011).

8. Masters, G., G. Laske, H. Bolton, A. Dziewonski, In ***Mineral Physics and Seismic Tomography***, pp. 63–87, S. Karato et al., Eds., American Geophysical Union, Washington DC (2000).

9. Youngs, B. A. R., G. A. Houseman, Formation of steep-sided topography from compositionally distinct dense material at the base of the mantle, ***J. Geophys. Res.***, **114**, B04404, doi:10.1029/2007JB005487 (2009).

6. Acknowledgements

The research was supported by the Hungarian Grant No. OTKA K-72665.